Supplementary information

Physical meaning of the parameters used in fractal kinetic and generalized adsorption models of Brouers-Sotolongo

Adsorption
Journal of the International Adsorption Society
ISSN: 0929-5607 (Print) 1572-8757 (Online)

Taher Selmi[a], Mongi Seffen[a], Habib Sammouda[a], Sandrine Mathieu[b], Jacek Jagiello[c], Alain Celzard[d] and Vanessa Fierro[d*]

[a] Laboratory of Energy and Materials (LabEM). High School of Sciences and Technology of Hammam Sousse – Sousse University, BP 4011, Hammam Sousse, Tunisia.

[b] Institut Jean Lamour, UMR Université de Lorraine – CNRS 7198, Parc de Saurupt, CS 50840, 54011 Nancy Cedex, France.

[c] Micromeritics Instrument Corporation, 4356 Communications Drive, Norcross, GA 30093, USA.

[d] Institut Jean Lamour, UMR Université de Lorraine – CNRS 7198, BP 21042, 88051 Epinal Cedex 9, France.

[*]Corresponding author (Vanessa Fierro)

Tel: + 33 372 74 96 77 Fax: + 33 372 74 96 38

E-mail address: Vanessa.Fierro@univ-lorraine.fr

Supplementary information

Table SI 1 shows the data obtained from the elemental analysis (EA) of all ACs used in this work. Carbon contents ranged from 84 to 90 wt. %, which is typical for this kind of materials. The carbon to hydrogen (C/H) ratio was the highest for F300. Higher oxygen contents were accompanied by higher hydrogen contents; thus, Cecalite® presented the highest oxygen and hydrogen contents.

Table SI 1: Chemical composition (wt. %) of the four activated carbons as obtained by EA

Samples	%N	%C	%H	%O	C/H
F200	0.37	86.21	0.51	5.49	169.04
F300	0.45	90.07	0.38	2.85	257.34
Acticarbone®	0.19	89.58	0.54	4.62	165.88
Cecalite®	0.23	84.21	0.85	7.30	99.07

Fig SI 1 shows weight losses and their derivatives (TGA and DTG curves, respectively) for the four ACs as a function of temperature in air flow. In general, TGA curves can be divided in two parts: in the first one, below 100°C, a minor weight loss (4-5 wt. %) is associated to moisture evolution or vaporisation of physically adsorbed water. In the second part of the curve, from 520°C to 730°C, a weight loss higher than 90% was observed, due to the complete combustion of the ACs in air. Above 700 – 800°C, only ashes remained (7 wt. %, on average). Similar results were found in the literature for activated carbons prepared from coconut shell (Tan et al. 2008).

The lower degradation temperature presented by Cecalite® (677°C) may be due to its lower carbon content and its higher oxygen content. The degradation temperatures of F200 and F300 samples were 687°C and 692°C, respectively, which are higher than that of Cecalite® and lower than of Acticarbone® (729°C). This behaviour is likely to be due to a combination of different facts: high carbon content, lowest fraction of narrow micropores (see

Erreur ! Source du renvoi introuvable.), and a nanotexture not so disordered as in most other samples (see Raman analysis below).

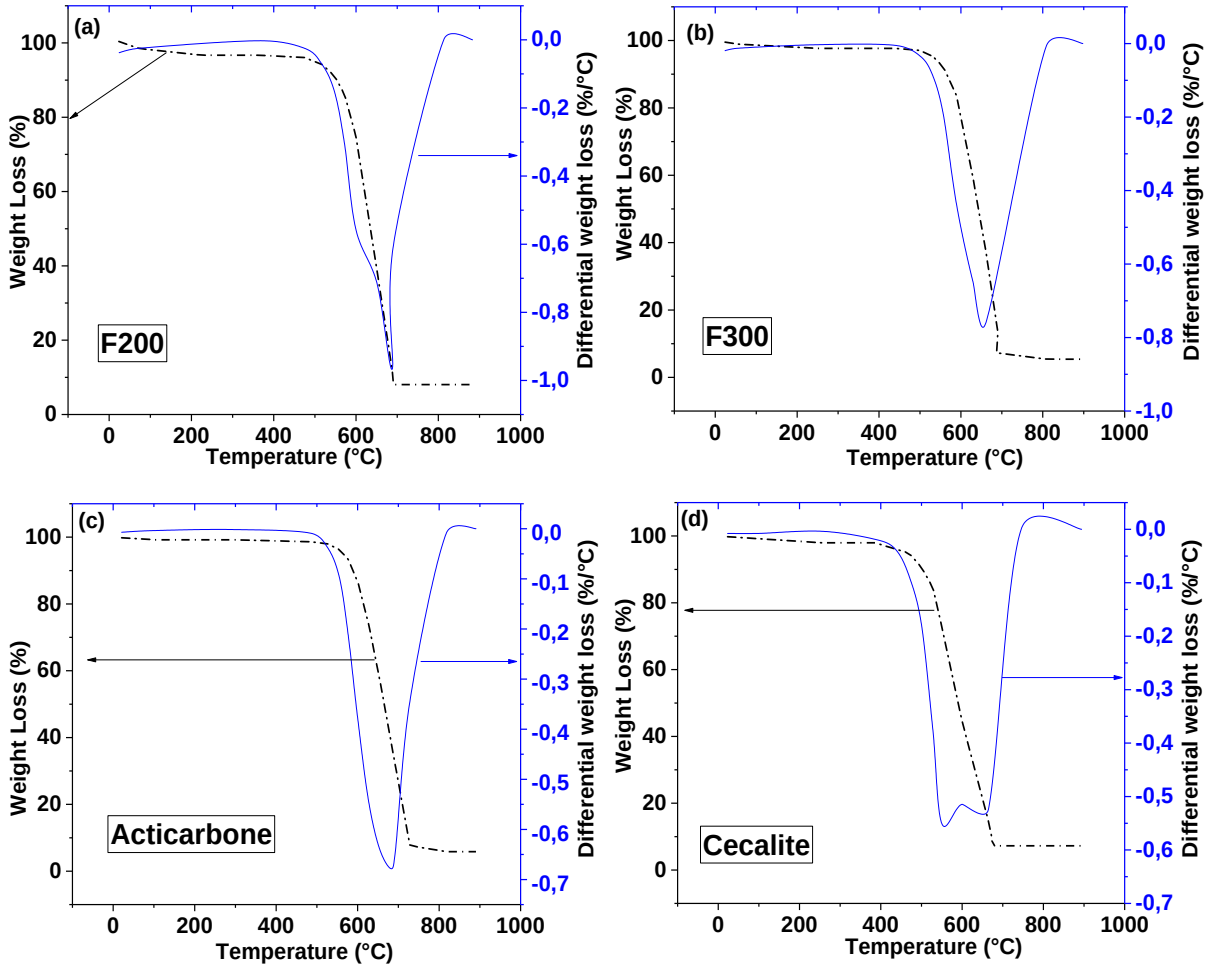

Fig SI 1 Raw and differential thermogravimetric curves of: (a) F200, (b) F300, (c) Acticarbone®, and (d) Cecalite®

Fig SI 2 shows the 1st-order Raman spectra of the four ACs, emphasising their D and G bands. All materials exhibited the typical features of highly disordered carbons, with an intense and broad D band around 1349 cm^{-1}, and a slightly narrower G band of rather similar intensity around 1606 cm^{-1}. Deconvolution of the spectra allowed calculating the corresponding I_D/I_G intensity ratios, equal to 2.63, 2.64, 2.46 and 2.94 for F300, F200, Acticarbone® and Cecalite®, respectively. Since such ACs are known to be non-graphitisable

carbons, higher I_D/I_G ratio means slightly larger crystallites, therefore Cecalite® should be the least disordered carbon of the series at the nanoscale (Ferrari et al. 2006).

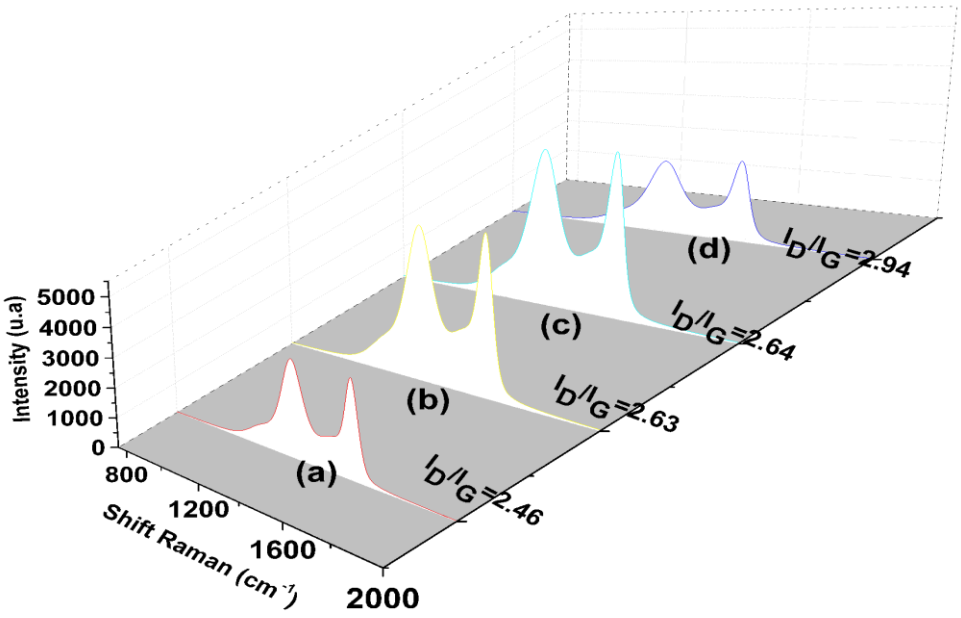

Fig SI 2 Raman spectra of all ACs: (a) Acticarbone®, (b) F300, (c) F200, and (d) Cecalite®. The intensity of D to G bands after deconvolution are given on the graph

Fig SI 3 shows the XRD patterns obtained for the four ACs. In all patterns, two broad bands were observed at 2θ around 25° and 45°. A fine peak can also be seen but is simply due to the sample holder. The first band centered on 2θ = 24.11°, 24.62°, 25.05° and 23.84°, respectively for F200, F300, Acticarbone® and Cecalite®, corresponds to the 002 reflexion of carbon, based on which the interlayer spacing, d002, could be calculated by application of Bragg's law. One finds 0.369, 0.361, 0.355 and 0.373 nm for F200, F300, Acticarbone® and Cecalite®, respectively. All these values are far higher than what is expected for perfect hexagonal graphite, 0.335 nm, further supporting the highly disordered nature of these carbonaceous materials.

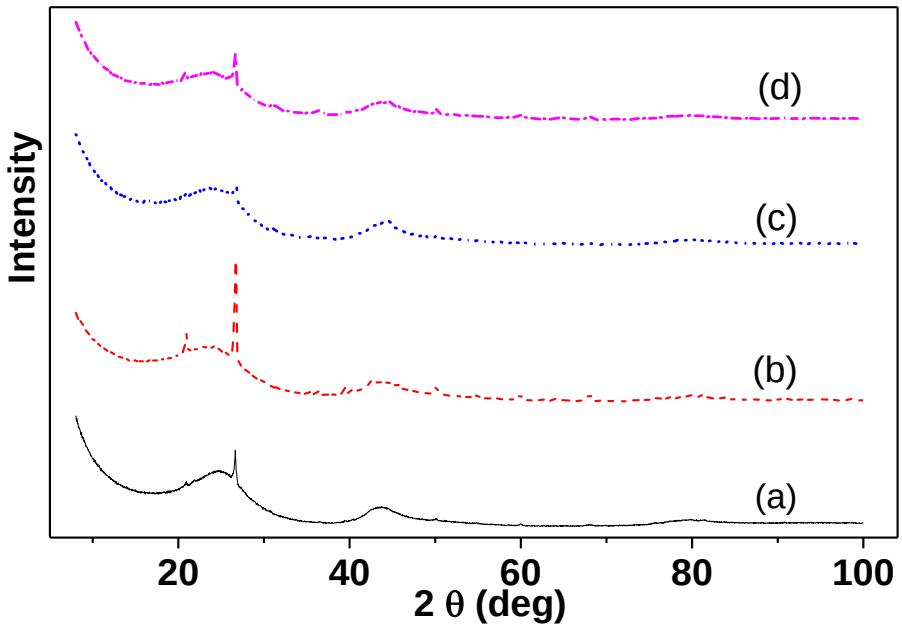

79

80 **Fig SI 3** XRD patterns of all ACs: (a) Acticarbone®, (b) Cecalite®, (c) F300, and (d) F200

81

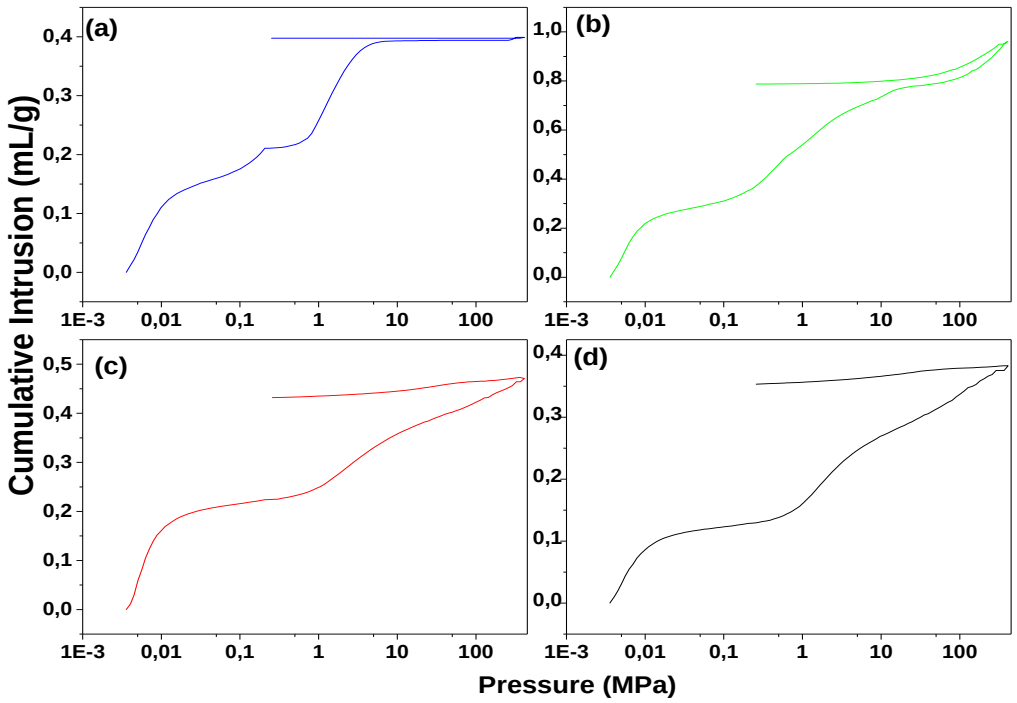

82

83 **Fig SI 4** Cumulative intrusion-extrusion curves of mercury in the four ACs: (a) Cecalite®, (b)

84 Acticarbone®, (c) F300, and (d) F200

85

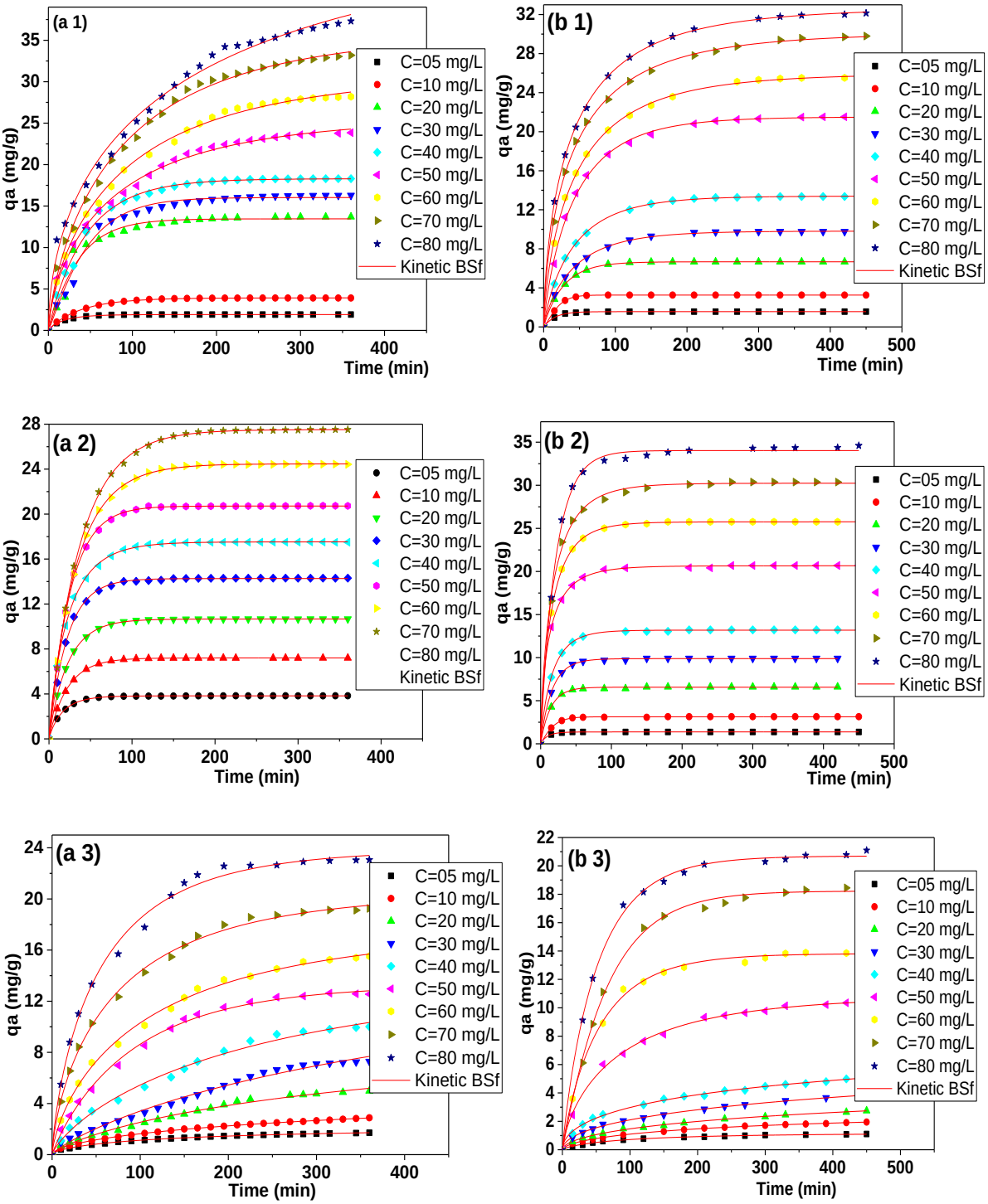

Fig SI 5 BSf (1,α) kinetics model applied to the adsorption of: (a) MB at pH 8, and (b) MO at pH 2.5 onto: (1) F200, (2) F300 and (3) Cecalite® samples for different initial concentrations at 25°C

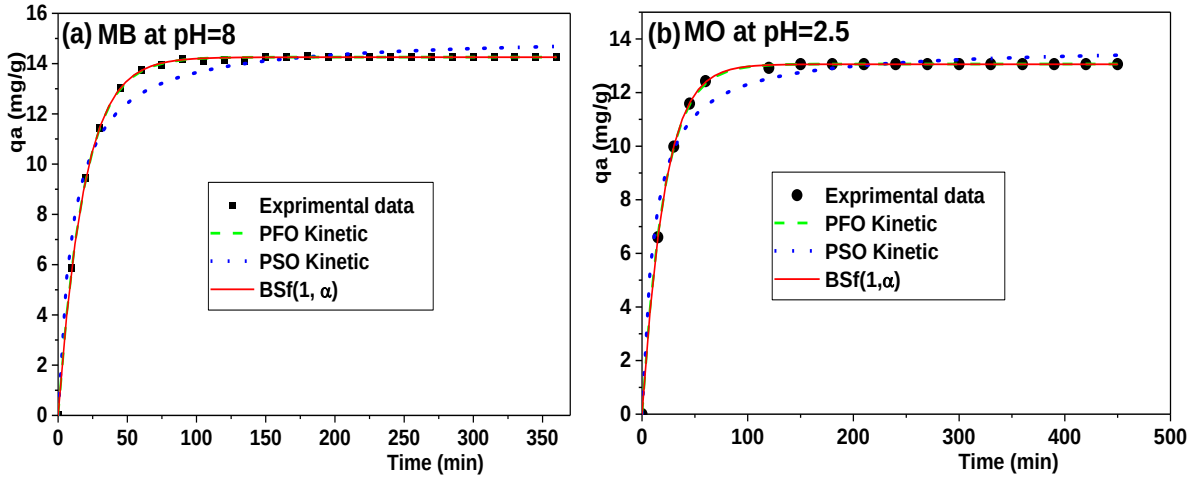

92

93 **Fig SI 6** Kinetics modelling of the adsorption onto Acticarbone® of: (a) MB at pH 8, and (b)
94 MO at pH 2.5 (C0 = 40 mg.L-1, 25°C)

95

96 **Table SI 2:** Activated carbons' porosity data derived from mercury porosimetry

	F200	F300	Acticarbone	Cecalite
Total Intrusion Volume (mL g^{-1})	0.52	0.45	1.09	0.43
Total Pore Area (m^2 g^{-1})	44	42	101	8
Median Pore Diameter (Volume) (µm)	94.8	2.3	2.3	1.4
Median Pore Diameter (Area) (µm)	0.0062	0.0060	0.0047	0.0041
Average Pore Diameter (4V/A) (µm)	48	44	44	217
Apparent Density (g mL^{-1})	1.26	1.20	1.08	1.44
Available porosity (%)	39.7	35.3	54.3	38.0
Percolation Fractal dimension	2.9	2.9	2.9	3.0
Backbone Fractal dimension	2.971	N/A	2.864	2.639
Permeability (mdarcy)	66.262	0.184	724.388	31.563

97

98

Table SI 3: Results of potentiometric titration: peak pKa and corresponding amounts of surface groups (expressed as mmol.g^{-1} in parentheses), pH_{PZC} and pHInitial of all ACs studied.

Samples	$pH_{initial}$	pK_a 3-5	pK_a 5-7	pK_a 7-9	pK_a 9-10	pK_a 10-12	Total amount (mmol.g^{-1})	pH_{PZC}
F200	6.73		5.08 (0.204)	7.40 (0.023)	9.76 (0.282)	10.61 (0.636)	1.145	7.20
F300	7.10		5.38 (0.076)			10.67 (0.529)	0.605	8.03
Acticarbone	7.03	4.73 (0.069)	6.41 (0.216)	8.38 (0.225)		11.09 (0.640)	1.150	7.36
Cecalite	6.82	4.62 (0.179)		7.89 (0.067)	9.52 (0.175)	10.99 (0.366)	0.787	7.75

Table SI 4: Effect of reaction order n on parameters of BSf kinetics model obtained by non-linear fit of the adsorption data of MB at pH 8 and MO at pH 2.5 onto F200 at 25°C.

BSf		Initial concentration of MB and MO (mg.L^{-1})											
		10			40			60			80		
		τ_C	α	R^2	τ_C	α	R^2	τ_C	α	R^2	τ_C	α	R^2
MB	n = 1	38.57	0.94	1.00	44.95	0.95	0.994	79.31	0.79	0.994	191.94	0.55	0.993
	n = 1.5	30.75	1.17	0.998	36.27	1.18	0.994	72.55	0.87	0.993	247.29	0.56	0.993
	n = 2	26.43	1.38	0.995	31.48	1.37	0.992	69.31	0.92	0.992	312.71	0.57	0.993
OM	n = 1	19.61	1.30	1.00	44.03	0.84	1.00	50.60	0.71	0.999	45.56	0.64	1.00
	n = 1.5	16.61	1.81	1.00	34.81	1.06	0.999	39.99	0.86	1.00	35.74	0.77	0.999
	n = 2	15.03	2.41	0.999	29.83	1.25	0.998	34.16	0.99	0.999	30.33	0.88	0.999

Table SI 5: Effect of reaction order n on parameters of BSf kinetics model obtained by non-linear fit of the adsorption data of MB at pH 8 and MO at pH 2.5 onto F300 at 25°C

BSf		Initial concentration of MB and MO ($mg.L^{-1}$)											
		10			40			60			80		
		τ_C	α	R^2	τ_C	α	R^2	τ_C	α	R^2	τ_C	α	R^2
MB	n = 1	16.69	0.92	1.00	22.18	0.99	0.999	25.68	1.02	0.999	37.82	0.97	1.00
	n = 1.5	13.28	1.25	0.999	17.74	1.32	1.00	20.55	1.34	0.999	30.19	1.22	0.999
	n = 2	11.50	1.61	0.998	15.32	1.65	0.999	17.73	1.66	0.998	25.99	1.46	0.998
OM	n = 1	16.78	1.13	0.999	17.33	0.85	0.999	17.28	0.77	1.00	21.42	0.96	0.998
	n = 1.5	14.17	1.62	0.999	13.97	1.20	1.00	13.79	1.10	0.999	17.38	1.30	0.999
	n = 2	12.93	2.20	0.999	12.36	1.59	0.999	12.12	1.47	0.999	15.28	1.69	1.00

Table SI 6: Effect of reaction order n on parameters of BSf kinetics model obtained by non-linear fit of the adsorption data of MB at pH 8 and MO at pH 2.5 onto Cecalite® at 25°C

BSf		Initial concentration of MB and MO ($mg.L^{-1}$)											
		10			40			60			80		
		τ_C	α	R^2	τ_C	α	R^2	τ_C	α	R^2	τ_C	α	R^2
MB	n = 1	596.60	0.58	1.00	251.24	0.78	0.993	119.95	0.72	0.998	59.34	0.76	0.995
	n = 1.5	877.43	0.59	0.999	314.53	0.79	0.992	118.05	0.77	0.997	49.62	0.87	0.993
	n = 2	1199.67	1.62	0.999	380.55	1.72	0.992	119.21	1.89	0.997	44.18	1.60	0.992
OM	n = 1	303.27	0.59	1.00	453.19	0.51	0.997	55.88	0.89	0.997	52.42	0.92	0.998
	n = 1.5	363.05	0.61	0.999	546.01	0.53	0.997	44.54	1.09	0.998	42.28	1.21	0.999
	n = 2	427.69	0.63	0.999	641.89	0.55	0.997	38.08	1.25	0.997	36.89	1.50	0.999

Table SI 7: Isotherm parameters of Freundlich, Jovanovich and Langmuir models fitted to the adsorption data of MB and MO at pH 8 and 2.5, respectively, and at 25°C.

Dyes	MB				MO			
Samples	F200	F300	Acticarbone	Cecalite	F200	F300	Acticarbone	Cecalite
Freundlich								
K_F	11.24	6.54	5.26	2.92	7.86	9.40	8.79	4.42
a	0.48	0.62	0.50	0.38	0.50	0.47	0.46	0.44
χ^2	4.07	10.16	5.31	0.34	1.39	7.73	10.48	1.95
R^2	0.963	0.867	0.906	0.977	0.989	0.940	0.919	0.971
Jovanovich								
$q_{e\,max}$	29.30	28.51	21.13	10.70	29.19	28.80	29.73	20.59
b	2.37	4.39	4.99	7.72	4.29	2.82	3.69	8.90
$Ce_{1/2}$	0.71	1.32	1.50	2.32	1.29	0.85	1.11	2.68
χ^2	0.16	5.24	1.91	1.67	1.88	1.09	0.41	0.47
R^2	0.998	0.931	0.966	0.888	0.985	0.992	0.997	0.993
Langmuir								
$q_{e\,max}$	38.24	42.37	27.85	12.38	37.28	35.94	37.50	25.57
b	2.58	6.18	5.76	5.74	4.46	2.92	3.88	8.86
R_L	0,03	0,07	0,07	0,07	0,05	0,04	0,05	0,10
$Ce_{1/2}$	2.58	6.18	5.76	5.74	4.46	2.92	3.88	8.86
χ^2	0.44	6.08	2.21	0.93	0.64	0.93	1.46	0.33
R^2	0.996	0.920	0.961	0.938	0.995	0.993	0.989	0.995